HHS Public Access

Author manuscript

NPJ Antimicrob Resist. Author manuscript; available in PMC 2024 September 12.

Published in final edited form as:

NPJ Antimicrob Resist. 2024 ; 2(1): . doi:10.1038/s44259-024-00040-9.

Sinefungin, a natural nucleoside analog of S-adenosyl methionine, impairs the pathogenicity of *Candida albicans*

Anushka Nayak,
Azam Khedri,
Alejandro Chavarria,
Kyla N. Sanders,
Homa Ghalei,
Sohail Khoshnevis✉
Department of Biochemistry, Emory University School of Medicine, Atlanta, GA, USA.

Abstract

Candida albicans, an opportunistic fungal pathogen, causes life-threatening infections in immunocompromised patients. Current antifungals are limited by toxicity, drug-drug interactions, and emerging resistance, underscoring the importance of identifying novel treatment approaches. Here, we elucidate the impact of sinefungin, an analog of S-adenosyl methionine, on the virulence of *C. albicans* strain SC5314 and clinical isolates. Our data indicate that sinefungin impairs pathogenic traits of *C. albicans* including hyphal morphogenesis, biofilm formation, adhesion to epithelial cells, and virulence towards *Galleria mellonella*, highlighting sinefungin as an avenue for therapeutic intervention. We determine that sinefungin particularly disturbs N6-methyladenosine (m^6A) formation. Transcriptome analysis of *C. albicans* hyphae upon sinefungin treatment reveals an increase in transcripts related to the yeast form and decrease in those associated with hyphae formation and virulence. Collectively, our data propose sinefungin as a potent molecule against *C. albicans* and emphasize further exploration of post-transcriptional control mechanisms of pathogenicity for antifungal design.

✉**Correspondence** and requests for materials should be addressed to Sohail Khoshnevis. skhoshn@emory.edu.

Author contributions

S.K. and A.N. designed the study. A.N., S.K., A.K., A.C. and K.S. performed experiments and acquired the data. A.N., S.K., A.C. and A.K. carried out data analysis and visualization. S.K., H.G., A.K. and A.N. interpreted the analysis. A.N. and S.K. drafted the manuscript. H.G., S.K. and A.N. edited the manuscript. All authors critically reviewed the manuscript and approved the final version of the manuscript.

Competing Interests

The authors declare no competing interests.

Supplementary information The online version contains supplementary material available at https://doi.org/10.1038/s44259-024-00040-9.

Candida albicans is a leading cause of nosocomial infection[1–3]. As an opportunistic fungal pathogen normally found on skin and mucosal surfaces, *C. albicans* is responsible for common conditions like oral thrush[4] and vaginal yeast infections[5], but can result in life-threatening systemic infections in immunocompromised patients. These infections, called candidiasis, are especially associated with high mortality rates in the ICU, where the most severe forms of infection have mortality rates exceeding 70%[3,6]. Due to rising resistance to existing antifungals, the high incidence (~750,000 cases per year) and mortality rates of candidiasis remain a major medical concern, highlighting the critical need to develop new strategies for combating *Candida spp*. infection[7,8].

The ability of *C. albicans* to invade deep tissues and organs for systemic infection is primarily attributed to the pathogen's morphological transition from single budding yeast cells to hyphal filaments in response to environmental stimuli[9–11]. This is the mechanism by which *C. albicans* adheres to host tissues and forms invasive biofilms, which is an important step in pathogenesis[12,13]. The transcriptional regulatory networks that control the switching from yeast to hyphae are well defined[14–18], but the post-transcriptional regulators that modulate this transition are less understood, and have largely been overlooked as therapeutic targets.

S-Adenosyl methionine (SAM) is the methyl donor for most known methyltransferases (MTases). Sinefungin, a natural nucleoside analog of SAM in which a sulfonium moiety is replaced by an amine, functions as a pan-inhibitor against SAM-dependent MTases (Fig. 1A)[19–23]. First iso-lated from cultures of *Streptomyces incarnatus* and *Streptomyces griseolus*, sinefungin has been shown to inhibit the development of various parasitic species, including *Trypanosoma*, *Leishmania*, and *Cryptosporidium* species, and has also demonstrated antifungal activity[19,24–27].

The antimicrobial properties of sinefungin can be attributed to its inhibition of transmethylation reactions, with adenine MTases and other DNA MTases exhibiting a particular sensitivity to sinefungin[20,27–29]. Prior studies have shown that sinefungin also inhibits MTases closely associated with post-transcriptional modification in *S. cerevisiae*, including cap MTase Abd1 and METTL3–14-WATP, a human ortholog of mRNA MTase Ime4[30–32].

In the current study, we determine the impact of sinefungin-mediated inhibition of transmethylation reactions on the virulence of *C. albicans* by evaluating treatment effects on the cellular morphological transition, surface adhesion, and biofilm formation. Our data indicated that sinefungin impairs pathogenic traits of *C. albicans* including hyphal lengthening, long-term biofilm formation, and adhesion to the human epithelial cell lines, without adversely affecting human cells. Furthermore, in vivo experiments showed that sinefungin treatment suppresses virulence of *C. albicans* in *Galleria mellonella*, therefore highlighting sinefungin as a potential avenue for therapeutic intervention in candidiasis. Interestingly, other SAM analogs did not demonstrate such effects on *C. albicans*. Comparing the methylation levels of proteins, metabolites, and nucleotides in the presence and absence of sinefungin revealed that the formation of N6-methyladenosine (m^6A) is particularly sensitive even to low concentrations of sinefungin. Global transcriptional

profiling of *C. albicans* hyphae upon treatment with sinefungin revealed that several transcripts associated with the yeast form of *C. albicans* are up-regulated whereas many virulence-associated genes are down-regulated. Together, our results underscore the importance of exploring post-transcriptional control mechanisms of pathogenicity for design of new antifungals.

Results

Sinefungin does not affect the growth of *Candida albicans* in the yeast form but inhibits hyphal growth and colony morphology at low concentrations

Sinefungin was originally identified as an antifungal agent and later was shown to impair the viability of multiple eukaryotic pathogens[19,20,24–27]. To test the effect of sinefungin on the growth of *C. albicans* in the planktonic form, we measured the growth rate of the strain SC5314 in the presence of varying concentrations of sinefungin. There was no significant change in the doubling time of the cells in the presence of sinefungin concentrations below 2 μM relative to no-drug condition (Fig. 1B). Cells exhibited slower growth in the presence of higher concentrations of sinefungin.

A key factor of *C. albicans* pathogenicity is its ability to switch from yeast to hyphae in response to environmental cues. To test if sinefungin inhibits transmethylation reactions required for the regulation of this transition, we evaluated the effect of sinefungin on hyphal morphogenesis. Sinefungin concentrations as low as 0.25 μM inhibited hyphae growth (Fig. 2A), with relative hyphae lengths significantly reduced ($p < 0.0001$) compared to the no drug group, 2 h after hyphal induction with FBS in nutrient-poor RPMI-1640 (Fig. 2B).

We next measured the effect of sinefungin on long-term hyphae formation. Wild-type *C. albicans* grown on solid spider media displayed a filamentous colony margin, representative of the yeast to hyphae transition. This phenotype was not present on plates with sinefungin concentrations of 0.5, 1 and 2 μM (Fig. 2C). Together, these data suggest that sinefungin inhibits both short-term and long-term hyphal growth in response to induction with serum and nutrient-poor conditions. This inhibitory effect is present at concentrations as low as 0.25 μM, despite sinefungin not influencing yeast growth rate until concentrations exceeded 2 μM.

Sinefungin inhibits *C. albicans* surface adhesion to polystyrene

Another component of *C. albicans* infection is surface adhesion, as planktonic yeast cells must adhere to surfaces before initiating tissue invasion and ultimately biofilm formation[33–35]. To analyze the effect of sinefungin on the initial stages of biofilm formation, we measured the adhesion of *C. albicans* to a polystyrene surface in the presence of varying concentrations of sinefungin. Our data show that *C. albicans* grown in the presence of 0.25 μM sinefungin in 96-well polystyrene plates have significantly impaired surface adhesion within 1 h ($p < 0.01$, Fig. 3A). The difference between treated and untreated cells becomes more prominent at 2 h ($p < 0.001$, Fig. 3A). These results indicate that cells grown in the presence of sinefungin are impaired in their ability to adhere to polystyrene in the early

stages of biofilm formation. Increasing the concentration of sinefungin above 0.5 μM did not increase its inhibitory effect on surface adhesion.

Next, we asked if long-term incubation with sinefungin could reverse the adhesion of pre-formed biofilms on polystyrene. *C. albicans* biofilms were grown in the absence of drug for 1.5 h, and then incubated with sinefungin for 18 h. We observed a clear reversal of adhesion, with 1 μM of sinefungin resulting in ~50% decrease in biofilm biomass ($p < 0.0001$, Fig. 3B). Furthermore, representative images of cells after 18 h of growth in the presence of sinefungin reveal that sinefungin successfully reverses adhesion to polystyrene after long-term periods of growth (Fig. 3B, C). This activity against adhered cells may prove useful in a clinical setting.

Sinefungin significantly reduces the adhesion of *C. albicans* to human epithelial cell lines without affecting epithelial cell viability

Because sinefungin could inhibit *C. albicans* adhesion to a polystyrene surface, we sought to study the impact of sinefungin on adhesion of *C. albicans* to two human epithelial cell lines that serve as effective substrates for cell adhesion: HEK293 (kidney) and H1299 (lung). In the presence of 0.5 μM sinefungin, the relative adhesion of *C. albicans* to both cell lines was reduced (Fig. 4A, B). Furthermore, increasing sinefungin concentration above 0.5 μM did not significantly strengthen this inhibitory effect.

Sinefungin's demonstrated capacity to suppress the morphological transition of *C. albicans* makes it a promising candidate for potential clinical application. To establish a range of sinefungin concentrations that retained antifungal properties against *C. albicans* without impacting human cell viability, we measured the metabolic activity and cell death of H1299 and HEK293T in the presence of varying concentrations of sinefungin. All tested concentrations of sinefungin had no noticeable effect on metabolic activity for both cell lines, indicating that low concentrations of sinefungin do not impact human epithelial cell proliferation (Fig. 5A, B). Sinefungin is also not cytotoxic against both cell lines at concentrations below 4 μM (Fig. 5C, D). Thus, though sinefungin is an MTase pan-inhibitor, it does not affect the viability of human epithelial cells at concentrations that inhibit the hyphal morphogenesis of *C. albicans*. These data suggest that there may be an MTase crucial to the cell-switching process for *C. albicans* that is highly sensitive to sinefungin compared to human SAM-dependent MTases.

Sinefungin impairs surface adhesion and adhesion to human epithelial cells in representative *C. albicans* clinical isolates

Because sinefungin shows a clear inhibitory effect on *C. albicans* reference strain SC5314, we evaluated the impact of sinefungin treatment on hyphal growth, adhesion, and biofilm formation of representative *C. albicans* clinical isolate stains. For isolates P76055 and P76067, which have been experimentally shown to be capable of forming hyphae under short-term growth conditions[36–38], a sinefungin concentration of 0.5 μM is sufficient to reduce surface adhesion to polystyrene 2 h after hyphal induction ($p < 0.0001$, Fig. 6A, B). Additionally, the isolates demonstrate decreased adhesion to human epithelial cell lines in the presence of 1 μM sinefungin after 2 h of incubation ($p < 0.001$, Fig. 6C, D). Again,

this inhibitory effect does not increase with increasing concentrations of sinefungin. We also tested if sinefungin could reverse the adhesion of preformed biofilms aftera long-term periodof growth for several *C. albicans* clinical isolates, P75010, P75016, P76055, P76067, and GC75, that vary in their abilities to form short-term hyphae and pseudohyphae[36–38]. After incubating preformed biofilms with sinefungin for 18 h, all five strains demonstrated a clear reversal of adhesion with significantly reduced biofilm biomass in treated groups relative to controls ($p < 0.01$, Fig. 6E). Together, these data confirm that the inhibitory effects of sinefungin on traits that mediate *C. albicans* pathogenicity are demonstrated across multiple strains of *C. albicans*, further implicating its unexplored therapeutic value.

Sinefungin has significant antifungal activity within in vivo *G. mellonella- C. albicans* infection model at biologically non-toxic concentrations

To assess the capacity of sinefungin to suppress virulence traits in vivo, we used the in vivo *G. mellonella* infection model. One hour after inoculation with *C. albicans, G. mellonella* was administered various concentrations of sinefungin via injection. Mortality counts were recorded daily. We found that for sinefungin concentrations 0.15 mg/kg, 0.76 mg/kg, and 3.81 mg/kg, over 60–80% of the larvae survived until the end of a 5-day observation period ($p < 0.0001$,Fig. 7A). Concentrations lower than 0.15 mg/kg likely do not have as high of an inhibitory effect on infection, resulting in higher mortality of *G. mellonella*. Notably, at sinefungin concentrations less than or equal to 0.76 mg/kg, we did not observe statistically significant toxicity to *G. mellonella*, indicatingthat sinefungin iseffective against *C. albicans* infection at concentrations lower than biologically non-toxic levels (Fig. 7B). Together, these data show that sinefungin is able to mitigate virulence in the *G. mellonella* infection model through its attenuation of pathogenic traits, highlighting its potential clinical applications.

Methylthioadenosine and adenosine dialdehyde, two other SAM analogs, do not affect surface adhesion in *C. albicans*

To test if the observed defects in the pathogenic traits of *C. albicans* in the presence of sinefungin are due to a general methyltransferase inhibition mechanism, we tested the effect of two other pan-methyltransferase inhibitors on biofilm formation by *C. albicans*. Adenosine dialdehyde (ADA) and 5′-methylthioadenosine (DMTA) are often used as cell permeable, global methyltransferase inhibitors[39]. Our analysis showed that unlike sinefungin, ADA and DMTA do not demonstrate the same inhibition of surface adhesion to polystyrene, suggesting that the antifungal activity of sinefungin is specific (Fig. 8).

Methylation profiling identifies m^{6}A mRNA modification as a major target of sinefungin in *C. albicans*

Sinefungin's strong inhibition of pathogenic traits of *C. albicans* at low concentrations without affecting yeast growth rate and human epithelial cell viability indicates that there may be an MTase that regulates the yeast-to-hyphae transition in *C. albicans* that is particularly sensitive to sinefungin. We hypothesize that despite being a known pan-MTase inhibitor, at concentrations below 2 μM, sinefungin specifically targets a form of methylation that is integral to hyphal morphogenesis without greatly affecting methylation patterns involved in other aspects of cellular growth and survival.

The major types of methylation in biological molecules involve protein methylation (mostly in the form of arginine or lysine methylation), nucleotide modifications (with m^6A and m^5C being the dominant methylated species in RNA and DNA, respectively), or the methylation of lipidsoluble metabolites. To explore which methylated moiety is the most sensitive to sinefungin, we profiled methylation levels in DNA, RNA, protein, and metabolites in *C. albicans* grown in the absence or presence of 0.5 and 1 μM of sinefungin in the hyphal form. Since the primary method for quantitative analysis of protein methylation is through enrichment by antibody[40], we probed arginine and lysine methylation with respective panmethyl antibodies. We did not observe a detectable change in the relative amounts of the most abundant methylated proteins in the cells treated with sinefungin relative to the control cells using Western Blot (Fig. 9A, B and Fig. S1). However, because this approach does not allow for quantification of low abundance proteins that may have been affected by the presence of sinefungin, further exploration of sinefungin's potential impact on the protein methylome is needed. Mass spectrometry-assisted analyses of the methylatedmetabolites in the presence or absence of sinefungin in hyphae cells did not reveal a significant change (Fig. 9C and Supplementary Data 1). While we did not observe any changes in the levels of m^5C in the presence of sinefungin (data not shown), we noticed that m^6A (N6-methyladenosine) levels in RNA were significantly reduced in groups treated with 0.5 μM and 1 μM of sinefungin (Fig. 9D). Together, these data suggest that m^6A levels in *C. albicans* RNAs are sensitive to sinefungin treatment.

RNA-sequencing of *C. albicans* treated with sinefungin reveals small pool of transcriptomic changes in genes related to hyphal growth and surface adhesion

To evaluate sinefungin's broader impact on signaling pathways that govern hyphal growth, cell adhesion, and biofilm formation, we analyzed overall transcriptomic changes in *C. albicans* after 2 h of hyphal growth with 1 μM sinefungin through mRNA sequencing. Out of over 10,000 transcripts screened (including two alleles for most genes), we identified 110 upregulated and 94 downregulated genes in the presence of sinefungin after comparison with a no drug control (Fig. 10A). GO term analysis of the affected cellular processes did not reveal a particularly vulnerable process, although many of the affected transcripts are linked to transport (Fig. 10B).

Among the downregulated pool, we found decreased expression of several genes associated with filamentation and pathogenetic traits of *C. albicans* including *SAP5*, *ECE1*, *DCK1, IHD1* and *HYR1* (Supplementary Data 2). Hyr1 and Ihd1 are two GPI-anchored proteins of hyphal cell wall required for virulence[41–43]. Notably, the transcript levels of several other GPI-anchored proteins are also reduced, including *PGA26*, *PGA63* and *PGA6*. Transcript level of Ahr1, a transcription factor involved in regulation of several virulence genes including Hsp90[44,45], was reduced as well. The transcript levels of several molecular chaperones, including Hsp90, Hsp104, and Ssa1 were also reduced. These molecular chaperones are very important for hyphal morphogenesis, biofilm formation, and host-cell invasion in response to temperature cues, and their inhibition leads to significantly reduced fungal virulence[46–50].

We identified several sinefungin-upregulated genes that decrease pathogenic traits when expressed in *C. albicans*, such as *YWP1*, *IFD6*, *CRZ2* and *HMX1* (Supplementary Data 2). GPI-anchored glycoprotein Ywp1 is present primarily in the yeast form of *C. albicans* and produces an antiadhesive effect, leading to markedly reduced biofilm adhesion when upregulated during hyphal growth conditions[51,52]. Alcohol dehydrogenase Ifd6 has been shown to inhibit biofilm matrix production processes closely related to biofilm formation[53]. Crz2 is a transcription factor that modulates the expression of many genes encoding mannosyltransferases and cell-wall proteins[54]. *CRZ2* overexpression confers resistance to acidic pH, alters cell-wall phosphomannan abundance, and interferes with pathways involved in protein glycosylation[54]. Hmx1 is a heme oxygenase which is induced by Hap1 in the presence of extracellular hemin and breaks down excess cytoplasmic heme[55,56]. Another Hap1 regulated gene, *FRP1*, encoding a ferric reductase-like proteins Frp1 necessary for heme utilization, is also overexpressed in the presence of sinefungin[56,57]. Together, these results suggest that sinefungin has an effect on the steady-state pool of several transcripts that are important for the pathogenicity of *C. albicans*.

Discussion

A strong link between hyphal morphogenesis and fungal pathogenesis has been highlighted in previous studies, with mutants lacking the ability to form hyphae demonstrating a severely impaired ability to form biofilms that are a key feature of *C. albicans* virulence[10,11,58]. Here, we show that MTase inhibitor sinefungin blocks hyphal morphogenesis in *C. albicans* at low concentrations without affecting yeast cell growth rate (Fig. 1). This observation suggests that the MTases which are mostly affected by sinefungin are not those critically active in the planktonic form of *C. albicans*, such as the mRNA-cap MTase ABD1. Therefore, to identify the targets of sinefungin, we focused our attention on the hyphae form. In addition to hyphal growth, sinefungin effectively prevented surface adhesion during early biofilm formation, reversed surface adhesion after biofilm formation, and reduced adhesion to human epithelial cells in *C. albicans* (Figs. 2–4, 6). Furthermore, sinefungin treatment at low, non-toxic concentrations dramatically improved survival of *G. mellonella* infected with *C. albicans*, showing strong potential for further exploration in therapeutic contexts (Fig. 7). Interestingly, methylation profiling of cells treated with sinefungin concentrations as low as 0.5 μM revealed that m^6A levels in RNA decrease in response to drug treatment, with all other evaluated forms of methylation showing little to no change in methylation levels at micromolar drug concentrations (Fig. 9). Though screens of transcription factor mutant networks have yielded extensive information about gene expression networks regarding the yeast-to-hyphae transition and eventual pathogenesis of *C. albicans*[14–18], the epigenetic mechanisms of control over cell plasticity are relatively unexplored[58,59]. DNA methylation in *C. albicans* is linked with phenotypic switching and transcriptional repression, with a two-fold difference in m^5C levels between hyphal and yeast forms observed in prior studies, suggesting that dynamic DNA methylation of structural genes may regulate transcriptional pathways that contribute to morphological plasicity[60,61]. In the context of post-transcriptional regulation, *C. albicans* hyphal morphogenesis has been linked to hyphal mRNA transport by SR-like RNA binding protein (Slr1), which is a serine-arginine rich protein that requires specific arginine

methylation patterns for effective intracellular localization[62]. Currently, post-transcriptional mechanisms of RNA methylation remains an underexplored area of the epigenetic networks that regulate hyphal morphogenesis. In other eukaryotic cell types, mRNA methylations, including m^6A modification, have been identified as key factors for various forms of cell differentiation[63–68]. Several reports on the function of m^6A show that it targets transcripts for degradation, facilitated by binding to YTH-domain containing proteins that deliver the transcripts to P bodies[69,70]. In *S. cerevisiae*, m^6A has mostly been studied in the context of meiosis[71,72]. In *C. albicans*, mRNA decay has been implicated as a major factor controlling hyphal morphogenesis, as mutations in cytoplasmic mRNA decay pathways have been shown to impair hyphal formation[61,73,74].

Given the sinefungin-mediated upregulation of certain hyphalsuppressed genes and downregulation of genes crucial for virulence and hyphal morphogenesis, sinefungin's antifungal activity may, in part, be due to inhibition of mRNA methylation processes that control hyphal gene expression (Fig. 10). Therefore, it is tempting to speculate that one of sinefungin's mechanisms of action may involve inhibition of posttranscriptional mRNA m^6A modifications. This is plausible given that adenine-specific MTases have been shown to be particularly sensitive to sinefungin-mediated inhibition[30–32]. m^6A is the most prevalent posttranscriptional modification of mRNA, related to mRNA stability, export, and decay[69,75,76]. As such, sinefungin's activity at sub-micromolar concentrations may be associated with targeted inhibition of an MTase which controls m^6A deposition in *C. albicans*, possibly the homolog of *S. cerevisae* Ime4[77,78], to in turn alter turnover of key mRNA transcripts involved in the yeast-to-hyphae transition. Sinefungin-mediated inhibition of this process can lead to upregulation of genes that are normally suppressed during hyphal growth and downregulation of genes that confer virulence traits to *C. albicans*. In line with this hypothesis, sinefungin treatment decreased the bulk m^6A levels in *C. albicans* hyphal RNAs (Fig. 9). However, sinefungin is a known pan-inhibitor of SAM-dependent MTases with many previously identified targets[21–23], so it is likely that sinefungin has multiple targets for inhibition which contribute to suppression of *C. albicans* virulence, though they have yet to be determined. Further investigation is underway to better elucidate specific targets of sinefungin in *C. albicans* at biologically relevant concentrations.

Most current antifungals target cell membrane and cell wall integrity (e.g., azoles interfere with ergosterol synthesis), but identifying new molecular therapy targets is becoming increasingly important with rise of antifungal drug resistance, which is why more work is needed to establish potential post-transcriptional targets for antifungals that block hyphal morphogenesis[79–81]. These data point to post-transcriptional modifications of mRNA as a possible component of sinefungin's antifungal mechanism, which is an avenue to be explored further. A compelling future investigation may involve elucidating the role of m^6A in hyphal morphogenesis in tandem with the results of this study. Biochemical and molecular genetics experiments are underway to better understand the relationship between sinefungin, m^6A, and hyphal development.

Methods

Effect of sinefungin on *C. albicans* yeast form growth

Sinefungin's activity against planktonic cells of SC5314 strain of *C. albicans* was tested by a broth microdilution method. Serially doublediluted concentrations of sinefungin were prepared in YPD medium, and 200 μL of each dilution was dispensed into the well of a presterilized, flat-bottomed 96-well microtiter plate (Thermo Scientific). SC5314 pre-cultures were grown overnight at 30 °C in YPD medium until stationary phase, and subsequently diluted to make day cultures. After growing to exponential phase, planktonic cells from the day cultures were dispensed in all experimental wells to reach a density of 1.2×10^6 cells/mL (equivalent to 0.1 OD_{600}) in a 200 μL working volume. For every tested concentration of sinefungin, four biological replicates were measured in microtiter plates incubated at 30 °C for 24 h in a microplate reader (BioTek). Optical density measurements were recorded on 20-min intervals to create a growth curve, from which doubling time for each treatment group was calculated using GraphPad Prism.

Effect of sinefungin on *C. albicans* hyphae length and surface adhesion to polystyrene

To test the impact of sinefungin on *C. albicans* growth in hyphal form, serially double-diluted concentrations of sinefungin were prepared in RPMI-1640 medium (Corning), and 200 μL of each dilution was dispensed into a 96 well polystyrene microtiter plate. Either SC5314 or clinical isolate strains P76055 and P76067 of *C. albicans* grown to exponential phase at 30 °C in YPD medium were dispensed in experimental wells to reach a density of 2.5×10^6 cells/mL (equivalent to 0.2 OD_{600}) for SC5314 or 1.3×10^6 cells/mL (equivalent to 0.1 OD_{600}) for the clinical isolates in a 200 μL working volume. Four biological replicates were measured for all concentrations tested. To examine cell growth at multiple timepoints during the early stages of biofilm formation, plates were incubated at 37 °C for either 1 hr or 2 h. For both respective timepoints, medium was aspirated from the wells at the end of incubation, and nonadherent cells were removed by washing twice with 200 μL sterile 1X phosphate buffered saline (PBS, Corning). Adherent cells were immobilized with 100 μL of methanol and dried at 37 °C for 10 min. Immobilized cells were stained with 1% crystal violet and imaged on a plate reader. Hyphal length was quantified using ImageJ software. Following imaging, 150 μL of 33% acetic acid was added to each well, and absorbance readings were recorded at 540 nm using a microplate reader to determine early biofilm biomass of each treated group.

Colony morphology assay on solid Spider media

Spider agar plates (1% Peptone, 1% D-Mannitol, and 0.2% K_2HPO_4) were prepared with no drug, 0.5 μM, or 1 μM sinefungin. SC5314 cells pre-grown overnight in YPD were serially diluted into YPD to a final concentration of 100 cells/mL, and 200 μL of cell suspension was spread onto the plates. Plates were incubated at 37 °C to induce hyphal growth for 5 days. Images of colony edges were obtained using the Leica M125 microscope.

Effect of sinefungin on long-term surface adhesion and biofilm reversal of *C. albicans*

To determine whether sinefungin reverses surface adhesion and inhibits biofilm formation over a long-term growth period, SC5314 or clinical isolate strains P75010, P75016, P76055, P76067, and GC75 grown overnight at 30 °C in YPD medium were diluted in Spider media to a density of 1.2×10^6 cells/mL. Biofilms were grown at 37 °C for 1.5 h in a polystyrene plate. At the end of incubation, the media was replaced with Spider media containing various concentrations of sinefungin, prepared through a serial double dilution method. Cells were then incubated for 18 h at 37 °C for long-term biofilm growth. Nonadherent cells were removed by washing twice with 200 μL sterile 1X PBS. The biofilm biomass of each treated group was measured using crystal violet as discussed before.

Infection capacity of sinefungin treated *C. albicans* against human epithelial cell lines

Two epithelial human cell lines, H1299 and HEK293, were cultured in RPMI-1640 and DMEM (Corning), respectively, with penicillinstreptomycin and 10% fetal bovine serum (FBS, Corning) in 24-well plates with ~100,000 cells/well. For H1299, serially double diluted concentrations of sinefungin were prepared in RPMI-1640, and SC5314 or clinical isolate strains P76055 and P76067, grown to exponential phase at 30 °C in YPD medium, were added to each dilution to create a cell density of about 10^6 cells/mL of *C. albicans* in the treated mediums right before incubation with the epithelial cells. For HEK293, sinefungin and *C. albicans* strains were prepared as previously described in DMEM. Once human cells reached 80–90% confluency, standard media was aspirated and replaced with 500 μL of their respective yeast and drug containing mediums. Plates were then incubated at 37 °C with 5% CO_2 and gentle shaking for 2 h. At the end of the incubation, media was aspired and each well was washed three times with 200 μL sterile PBS to remove nonadherent yeast from the wells. All remaining human and *C. albicans* cells were detached from wells with 0.25% Trypsin-EDTA (Gibco), placed in microcentrifuge tubes and spun down for 10 s at max speed. Cell pellets were resuspended in 1 mL of YPD medium. 100 μL of cell suspension was dispensed into a 96-well microtiter plate, with three technical replicates for each experimental group. The plate was incubated at 30 °C overnight while shaking in a microplate reader to record optical density on 20-min intervals. Optical density values after 6–8 h of growth were used to quantify the amount of invading SC5314 cells at each drug concentration and normalized to no drug condition to calculate relative infection rate.

Cytotoxicity of sinefungin against human epithelial cell lines

H1299 and HEK293 were cultured in RPMI-1640 and DMEM, respectively, with penicillin-streptomycin and 10% FBS in 24-well plates. Serially double diluted concentrations of sinefungin were prepared in RPMI-1640 for the H1299 assay, or DMEM for the HEK293 assay. Once cells reached 80–90% confluency, media was aspirated and replaced with 500 μL of prepared media containing varying concentrations of sinefungin. Cells were incubated for 24 h at 37 °C and cell death was measured through a lactate dehydrogenase (LDH) assay using the CytoTox 96 kit (Promega). For each experiment, full lysis was obtained from treating cells with lysis buffer for 30 min prior to the LDH assay. Lysed cells were used as a reference for 100% cytotoxicity, to which all values were normalized.

Metabolic activity of human epithelial cells in the presence of sinefungin

H1299 and HEK293 were cultured in RPMI-1640 and DMEM, respectively, with penicillin-streptomycin and 10% FBS in 24-well plates. Serially double diluted concentrations of sinefungin were prepared in RPMI-1640 for the H1299 assay, or DMEM for the HEK293 assay. Once cells reached 80–90% confluency, standard media was aspirated and replicated with 500 μL of prepared media containing varying concentrations of sinefungin. Cells were incubated for 24 h at 37 °C and their metabolic activity was measured through a cell proliferation (CCK-8) assay (Dojindo).

Protein methylation profiling for *C. albicans* after sinefungin treatment

SC5314 cells were grown for 2 h at 37 °C in RPMI-1640 with 10% FBS to form fhyphae in the presence of varying concentrations of sinefungin. Total protein was extracted from harvested cells by resuspending cells in a solution of SUMEB sample buffer (1% SDS, 8 M urea, 10 mM MOPS pH 6.8, 10 mM EDTA, 0.01% bromophenol blue) containing 15% β-mercaptoethanol, 1% pepstatin, 1 mM E-64, and 1 mM phenylmethylfsulfonyl fluoride (PMSF). Cells were then vortexed thrice with silica disruption beads (RPI), with 1 min of vortexing at 4 °C and then 1 min of rest on ice. Proteins were resolved on 12% SDS-PAGE gels, transferred to nitrocellulose, and immunoblotted using antibodies against mono- and dimethyl arginine or mono-, di-, and tri-methyl lysine (Abclonal). Anti-GAPDH-HRP was used to measure even loading.

DNA methylation profiling for *C. albicans* after sinefungin treatment

For DNA analysis, cells were grown as before and the total gDNA was extracted using phenol:chloroform:isoamyl alcohol (25:24:1). The DNA-containing aqueous phase was separated from the organic phase by centrifugation. DNA was precipitated by addition of ethanol followed by centrifugation. Pelleted DNA was resuspended in Tris-EDTA (TE) buffer and incubated with RNase A for 15 min at 42 °C before storage at −20 °C. 5 μg total DNA was spotted on HiBond Nylon membrane using a dot-blot apparatus. DNA was crosslinked to the membrane at 256 nM using a crosslinker (Stratalinker). The membrane was blocked with 3% milk solution in TBS-T. m^5C was probed using an anti-m^5C primary antibody (Abclonal) and anti-rabbit HRP-conjugated secondary antibody.

RNA methylation profiling after sinefungin treatment

For RNA m^6A content analysis, total RNA was extracted using hot phenol method followed by precipitation with ethanol and sodium acetate overnight at −20 °C. The precipitated RNA was collected by centrifugation. DNA was digested using DNase I (NEB), and the digested DNA and the DNase I were further removed using an RNA purification kit (Zymo Research). 5 μg total RNA was denatured at 65 °C and spotted on HiBond Nylon membrane using a dot-blot apparatus. After UV-crosslinking and blocking with 3% milk solution in TBS-T, m^6A was probed using an anti m^6A primary antibody (Active Motif) and anti-rabbit HRP-conjugated secondary antibody.

Metabolite methylation profiling after sinefungin treatment

Sample preparation: The cell pellet, containing 5 million cells, was homogenized in 200 μL PBS using a Bead Ruptor (Omni international, Kennesaw, GA). Metabolites were extracted from the homogenized sample with 4 times the volume (800 μL) of 1:1 mixture of Acetonitrile:Methanol (ACN:MeOH). Samples were subsequently vortexed for 3 s and incubated on ice for 30 min. The samples were then centrifuged at 20,000 × *g* for 10 min to pellet precipitated protein. Finally, the supernatant was filtered through a 0.2 μm filter and dried under nitrogen gas and then reconstituted in 200 μL water: Acetonitrile (1:4), vortexed, and centrifuged for 2 min at 13,000 rpm prior to LC-MS analysis. A quality control (QC) sample was prepared by pooling an aliquot of each sample and prepped in the same manner as the samples, as were sample blanks (ACN:MeOH). The external standard consisted of leucine and Isoleucine (Sigma-Aldrich, St. Louis, MO)and was prepared at a final concentration in the range 0.0078 μg/mL–1 μg/mL.

Metabolomics data were acquired using an Agilent Infinity II/6495 LC-MS/MS fitted with an InfinityLab Poroshell 120 HILIC-Z column (Agilent, 2.1 × 150 mm, 2.7 Micron). The mass spectrometer was operated in both positive and negative ion modes using polarity switching. The mobile phase was 100% water with 20 mM ammonium acetate, 5 μM Medronic acid (mobile phase A), and 100% Acetonitrile (mobile phase B). The chromatographic method used the gradient program depicted in Supplementary Data 3. The column temperature was set to 15 °C, and the injection volume was 2 μL. For mass spectrometry analysis, the gas temperature for the source was operated at 200 °C, the gas flow was 14 L/min, with nebulizer of 50 psi sheath gas temperature was 375 °C, sheath gas flow was 12 L/min. The capillary for the positive ion mode was set to 3000 V, and 2500 V for the negative ion mode. The pressure RF for the iFunnel was set with range of 60 V to 150 V for both positive and positive ion mode.

Skyline (version 22.2) was used to process all raw LC-MS data. Leucine and Isoleucine were used as the external standard curve. All concentration point should be linear portion of the curve with an R-squared value no less than 0.9. Additionally, the data is normalized by using SERRF, a QC-based sample normalization method which uses Random Forest algorithm to correct the systematical error such as batch effect, day-to-day variation, etc. coefficient of variation of QCs was also generated to evaluate the performance.

Effect of alternative SAM analogs on SC5314 surface adhesion to polystyrene

To observe the effect of alternative SAM analogs on *C. albicans* growth in hyphal form, serially double-diluted concentrations of adenosine dialdehyde (ADA) and 5'-deoxy-5'-methylthioadenosine (DMTA) in 1% DMSO were prepared in RPMI-1640 medium, and 200 μL of each dilution was dispensed into a 96 well microtiter plate. SC5314 grown to mid-log phase at 30 °C in YPD medium was dispensed in experimental wells to reach a density of 1.2×10^6 cells/mL in a 200 μL working volume. Plates were incubated at 37 °C for 3 h. Medium was aspirated from the wells at the end of incubation, and nonadherent cells were removed by washing twice with 200 μL sterile 1X phosphate buffered saline (PBS). The biofilm biomass of each treated group was measured using crystal violet as discussed before.

Effect of sinefungin on SC5314 virulence towards *G. mellonella*

Twenty healthy *G. mellonella* larvae during their final larval stage were specifically selected to have uniform size, approximately 0.2 g, and ensured to lack any gray markings. SC5314 grown to exponential phase at 30 °C in YPD medium were collected, washed with PBS, and then used to create inoculums of 10^5 CFU/larva. *C. albicans* was administered to *G. mellonella* in volumes of 10 μL, with a control group receiving an equal volume of water (sinefungin solvent). One hour after inoculation, sinefungin at various concentrations was administered via injection into the last right pro-leg. Following the injection, the larvae were placed in plastic petri dishes and kept at 37 °C, and daily mortality counts were recorded.

Toxicity of sinefungin against G. mellonella

Sinefungin was administered to *G. mellonella* at concentrations of 0.006, 0.03, 0.15, 0.76, 3.81, 19 and 95.34 mg/kg in water, with a control group receiving an equal volume of water. Following the injection, the larvae were placed in plastic petri dishes and kept at a temperature of 37 °C, and daily mortality counts were recorded.

mRNA-Seq of *C. albicans* after sinefungin treatment during hyphal growth

SC5314 cells were grown in hyphae form (37 °C, RPMI-1640 with 10% FBS) for 2 h in the presence or absence of 1 μM sinefungin. Total RNA was extracted using hot phenol method followed by precipitation with ethanol and sodium acetate overnight at −20 °C. The precipitated RNA was collected by centrifugation. DNA was digested using DNase I (NEB), and the digested DNA and the DNase I were further removed using an RNA purification kit (Zymo Research). mRNA was purified from total RNA using poly-T oligo-attached magnetic beads. After fragmentation, the first strand cDNA was synthesized using random hexamer primers, followed by the second strand cDNA synthesis (Novogene). Sequencing reads were aligned to *C. albicans* reference (Assembly 22) using Hisat2 v2.0.5[82]. Differential expression analysis of two conditions (three biological replicates per condition) was performed using the DESeq2R package version 1.20.0[83]. Gene Ontology (GO) enrichment analysis was carried out using the GO Term Finder and GO Slim Mapper tools from the Candida Genome Database (CGD)[84,85]. Raw sequencing reads (RNA-seq) from this study have been submitted to the NCBI sequence read archive (SRA) under BioProject accession number PRJNA1114783.

Supplementary Material

Refer to Web version on PubMed Central for supplementary material.

Acknowledgements

We thank members of Khoshnevis Lab for critically reading this manuscript. We thank Landon Burton and Nickan Khoshnevis for technical assistance. This work was supported by the National Institute of Health (1R35GM150760), CF-AIR Center Pilot Grant and Emory University Research Council (URC) grants to S.K. and the National Institute of Health (5R35GM138123) to H.G. This work was supported by the Emory University Integrated Metabolomics and Lipidomics Core Facility (RRID:SCR_023527).

Data availability

The dataset supporting the conclusions of this article are included within the article and supplementary information. Raw sequencing reads from RNA-seq data of SC5314 treated with sinefungin are available in the NCBI Sequence Read Archive under BioProject accession number PRJNA1114783.

References

1. Pal M, Hofmeister M, Gutama KP, Paula CR & Leite DP Growing role of *Candida albicans* as an important cause of nosocomial infection. J. Adv. Microbiol. Res 3, 47–52 (2022).
2. Perlroth J, Choi B & Spellberg B Nosocomial fungal infections: epidemiology, diagnosis, and treatment. Med. Mycol 45,321–346(2007). [PubMed: 17510856]
3. Pappas PG et al. A prospective observational study of candidemia: epidemiology, therapy, and influences on mortality in hospitalized adult and pediatric patients. Clin. Infect. Dis 37, 634–643 (2003). [PubMed: 12942393]
4. Lu SY Oral candidosis: pathophysiology and best practice for diagnosis, classification, and successful management. J. Fungi 7. 10.3390/jof7070555 (2021).
5. Willems HME, Ahmed SS, Liu J, Xu Z & Peters BM Vulvovaginal candidiasis: a current understanding and burning questions. J. Fungi 6. 10.3390/jof6010027 (2020).
6. Schroeder M et al. Epidemiology, clinical characteristics, and outcome of candidemia in critically ill patients in Germany: a singlecenter retrospective 10-year analysis. Ann. Intensive Care 10, 142 (2020). [PubMed: 33064220]
7. Bongomin F, Gago S, Oladele RO & Denning DW Global and multi-national prevalence of fungal diseases-estimate precision. J. Fungi 3. 10.3390/jof3040057 (2017).
8. Vitiello A et al. Antifungal drug resistance: an emergent health threat. Biomedicines 11. 10.3390/biomedicines11041063(2023).
9. Chow EWL, Pang LM & Wang Y From Jekyll to Hyde: the yeasthyphal transition of *Candida albicans*. Pathogens 10. 10.3390/pathogens10070859 (2021).
10. Saville SP, Lazzell AL, Monteagudo C & Lopez-Ribot JL Engineered control of cell morphology in vivo reveals distinct roles for yeast and filamentous forms of *Candida albicans* during infection. Eukaryot. Cell 2, 1053–1060 (2003). [PubMed: 14555488]
11. Lo HJ et al. Nonfilamentous *C. albicans* mutants are avirulent. Cell 90, 939–949 (1997). [PubMed: 9298905]
12. Uppuluri P, Pierce CG & Lopez-Ribot JL *Candida albicans* biofilm formation and its clinical consequences. Future Microbiol. 4, 1235–1237 (2009). [PubMed: 19995182]
13. Nobile CJ & Mitchell AP Genetics and genomics of *Candida albicans* biofilm formation. Cell Microbiol. 8, 1382–1391 (2006). [PubMed: 16848788]
14. Nobile CJ et al. A recently evolved transcriptional network controls biofilm development in *Candida albicans*. Cell 148, 126–138 (2012). [PubMed: 22265407]
15. Homann OR, Dea J, Noble SM & Johnson AD A phenotypic profile of the Candida albicans regulatory network. PLoS Genet. 5, e1000783 (2009). [PubMed: 20041210]
16. Finkel JS et al. Portrait of *Candida albicans* adherence regulators. PLoS Pathog. 8, e1002525 (2012). [PubMed: 22359502]
17. Perez JC, Kumamoto CA & Johnson AD *Candida albicans* commensalism and pathogenicity are intertwined traits directed by a tightly knit transcriptional regulatory circuit. PLoS Biol. 11, e1001510 (2013). [PubMed: 23526879]
18. Pukkila-Worley R, Peleg AY, Tampakakis E & Mylonakis E *Candida albicans* hyphal formation and virulence assessed using a Caenorhabditis elegans infection model. Eukaryotic Cell. 8, 1750–1758 (2009). [PubMed: 19666778]
19. Hamil RL & Hoehn MM A9145, a new adenine-containing antifungal antibiotic. I. Discovery and isolation. J. Antibiot 26, 463–465 (1973).

20. Barbes C, Sanchez J, Yebra MJ, Robert-Gero M & Hardisson C Effects of sinefungin and S-adenosylhomocysteine on DNA and protein methyltransferases from Streptomyces and other bacteria. FEMS Microbiol. Lett 57, 239–243 (1990). [PubMed: 2210336]
21. Zhang J & Zheng YG SAM/SAH analogs as versatile tools for SAM-dependent methyltransferases. ACS Chem. Biol 11, 583–597 (2016). [PubMed: 26540123]
22. Fischer TR et al. Chemical Biology and medicinal chemistry of RNA methyltransferases. Nucleic Acids Res. 50, 4216–4245 (2022). [PubMed: 35412633]
23. Yebra MJ et al. The effect of sinefungin and synthetic analogues on RNA and DNA methyltransferases from Streptomyces. J. Antibiot 44, 1141–1147 (1991).
24. Nolan LL Molecular target of the antileishmanial action of sinefungin. Antimicrob. Agents Chemother 31, 1542–1548 (1987). [PubMed: 3124733]
25. Bhattacharya A et al. Genomewide analysis of mode of action of the S-Adenosylmethionine analogue Sinefungin in Leishmania infantum. mSystems 4. 10.1128/mSystems.00416-19 (2019).
26. Brasseur P, Lemeteil D & Ballet JJ Curative and preventive anticryptosporidium activities of sinefungin in an immunosuppressed adult rat model. Antimicrob. Agents Chemother 37, 889–892 (1993). [PubMed: 8494386]
27. Gordee RS & Butler TF A9145, a new adenine-containing antifungal antibiotic. II. Biological activity. J. Antibiot 26, 466–470 (1973).
28. Fuller RW & Nagarajan R Inhibition of methyltransferases by some new analogs of S-adenosylhomocysteine. Biochem. Pharm 27, 1981–1983 (1978). [PubMed: 708481]
29. Schluckebier G, Kozak M, Bleimling N, Weinhold E & Saenger W Differential binding of S-adenosylmethionine S-adenosylhomocysteine and Sinefungin to the adenine-specific DNA methyltransferase M.TaqI. J. Mol. Biol 265, 56–67 (1997). [PubMed: 8995524]
30. Chrebet GL et al. Cell-based assays to detect inhibitors of fungal mRNA capping enzymes and characterization of sinefungin as a cap methyltransferase inhibitor. J. Biomol. Screen 10, 355–364 (2005). [PubMed: 15964937]
31. Zheng S et al. Mutational analysis of Encephalitozoon cuniculi mRNA cap (guanine-N7) methyltransferase, structure of the enzyme bound to sinefungin, and evidence that cap methyltransferase is the target of sinefungin's antifungal activity. J. Biol. Chem 281, 35904–35913 (2006). [PubMed: 16971388]
32. Selberg S et al. Discovery of small molecules that activate RNA methylation through cooperative binding to the METTL3–14-WTAP complex active site. Cell Rep. 26, 3762–3771.e3765 (2019). [PubMed: 30917327]
33. McCall AD, Pathirana RU, Prabhakar A, Cullen PJ & Edgerton M *Candida albicans* biofilm development is governed by cooperative attachment and adhesion maintenance proteins. NPJ Biofilms Microbiomes 5, 21 (2019). [PubMed: 31452924]
34. Farrell SM, Hawkins DF & Ryder TA Scanning electron microscope study of Candida albicans invasion of cultured human cervical epithelial cells. Sabouraudia 21, 251–254 (1983). [PubMed: 6356411]
35. Moyes DL, Richardson JP & Naglik JR *Candida albicansepithelial* interactions and pathogenicity mechanisms: scratching the surface. Virulence 6, 338–346 (2015). [PubMed: 25714110]
36. Huang MY et al. Circuit diversification in a biofilm regulatory network. PLoS Pathog. 15, e1007787 (2019). [PubMed: 31116789]
37. Glazier VE et al. The Candida albicans reference strain SC5314 contains a rare, dominant allele of the transcription factor Rob1 that modulates filamentation, biofilm formation, and oral commensalism. mBio 14, e01521–23, 10.1128/mbio.01521-23 (2023). [PubMed: 37737633]
38. Tucey TM et al. Metabolic competition between host and pathogen dictates inflammasome responses to fungal infection. PLoS Pathog. 16, e1008695 (2020). [PubMed: 32750090]
39. Cheng D, Vemulapalli V & Bedford MT Chapter Four – Methods applied to the study of protein arginine methylation. Methods Enzymol. 512, 71–92 (2012). [PubMed: 22910203]
40. Lund PJ, Lehman SM & Garcia BA Chapter Twenty – Quantitative analysis of global protein lysine methylation by mass spectrometry. Methods Enzymol. 626, 475–498 (2019). [PubMed: 31606088]

41. Bailey DA et al. The *Candida albicans HYR1* gene, which is activated in response to hyphal development, belongs to a gene family encoding yeast cell wall proteins. J. Bacteriol 178, 5353–5360 (1996). [PubMed: 8808922]
42. De Groot PW, Hellingwerf KJ & Klis FM Genome-wide identification of fungal GPI proteins. Yeast 20, 781–796 (2003). [PubMed: 12845604]
43. Nantel A et al. Transcription profiling of *Candida albicans* cells undergoing the yeast-to-hyphal transition. Mol. Biol. Cell 13, 3452–3465 (2002). [PubMed: 12388749]
44. Askew C et al. The zinc cluster transcription factor Ahr1p directs Mcm1p regulation of *Candida albicans* adhesion. Mol. Microbiol 79, 940–953 (2011). [PubMed: 21299649]
45. Diezmann S et al. Mapping the Hsp90 genetic interaction network in Candida albicans reveals environmental contingency and rewired circuitry. PloS Genet. 8, e1002562 (2012). [PubMed: 22438817]
46. O'Meara TR, Robbins N & Cowen LE The Hsp90 Chaperone Network Modulates Candida Virulence Traits. Trends Microbiol. 25, 809–819 (2017). [PubMed: 28549824]
47. Robbins N & Cowen LE Roles of Hsp90 in *Candida albicans* morphogenesis and virulence. Curr. Opin. Microbiol 75, 102351, 10.1016/j.mib.2023.102351 (2023). [PubMed: 37399670]
48. Neves-da-Rocha J et al. Insights and perspectives on the role of proteostasis and heat shock proteins in fungal infections. Microorganisms 11. 10.3390/microorganisms11081878 (2023).
49. Fiori A et al. The heat-induced molecular disaggregase Hsp104 of *Candida albicans* plays a role in biofilm formation and pathogenicity in a worm infection model. Eukaryot. Cell 11, 1012–1020 (2012). [PubMed: 22635920]
50. Sun JN et al. Host cell invasion and virulence mediated by Candida albicans Ssa1. PLoS Pathog. 6, e1001181 (2010). [PubMed: 21085601]
51. Granger BL Insight into the antiadhesive effect of yeast wall protein 1 of *Candida albicans*. Eukaryot. Cell 11, 795–805 (2012). [PubMed: 22505336]
52. Granger BL et al. Yeast wall protein 1 of *Candida albicans*. Microbiology 151, 1631–1644 (2005). [PubMed: 15870471]
53. Nobile CJ et al. Biofilm matrix regulation by *Candida albicans* Zap1. PLoS Biol. 7, e1000133 (2009). [PubMed: 19529758]
54. Znaidi S et al. Systematic gene overexpression in *Candida albicans* identifies a regulator of early adaptation to the mammalian gut. Cell. Microbiol 20, e12890 (2018). [PubMed: 29998470]
55. Santos R et al. Haemin uptake and use as an iron source by *Candida albicans*: role of Ca*HMX1*-encoded haem oxygenase. Microbiology 149, 579–588 (2003). [PubMed: 12634327]
56. Andrawes N et al. Regulation of heme utilization and homeostasis in Candida albicans. PLoS Genet. 18, e1010390 (2022). [PubMed: 36084128]
57. Roy U et al. Ferric reductase-related proteins mediate fungal heme acquisition. eLife 11, e80604, 10.7554/eLife.80604 (2022). [PubMed: 36200752]
58. Kadosh D Control of *Candida albicans* morphology and pathogenicity by post-transcriptional mechanisms. Cell Mol. Life Sci 73, 4265–4278 (2016). [PubMed: 27312239]
59. Verma-Gaur J & Traven A Post-transcriptional gene regulation in the biology and virulence of *Candida albicans*. Cell Microbiol. 18, 800–806 (2016). [PubMed: 26999710]
60. Mishra PK, Baum M & Carbon J DNA methylation regulates phenotype-dependent transcriptional activity in *Candida albicans*. Proc. Natl Acad. Sci. USA 108, 11965–11970 (2011). [PubMed: 21730141]
61. Russell PJ, Welsch JA, Rachlin EM & McCloskey JA Different levels of DNA methylation in yeast and mycelial forms of *Candida albicans*. J. Bacteriol 169, 4393–4395 (1987). [PubMed: 3305486]
62. Ariyachet C et al. Post-translational modification directs nuclear and hyphal tip localization of *Candida albicans* mRNA-binding protein Slr1. Mol. Microbiol 104, 499–519 (2017). [PubMed: 28187496]
63. Agarwala SD, Blitzblau HG, Hochwagen A & Fink GR RNA methylation by the MIS complex regulates a cell fate decision in yeast. PLoS Genet. 8, e1002732 (2012). [PubMed: 22685417]

64. Song T et al. Zfp217 mediates m6A mRNA methylation to orchestrate transcriptional and post-transcriptional regulation to promote adipogenic differentiation. Nucleic Acids Res. 47, 6130–6144 (2019). [PubMed: 31037292]
65. Popis MC, Blanco S & Frye M Posttranscriptional methylation of transfer and ribosomal RNA in stress response pathways, cell differentiation, and cancer. Curr. Opin. Oncol 28, 65–71 (2016). [PubMed: 26599292]
66. Hongay CF & Orr-Weaver TL Drosophila Inducer of Meiosis 4 (IME4) is required for Notch signaling during oogenesis. Proc. Natl Acad. Sci. USA 108, 14855–14860 (2011). [PubMed: 21873203]
67. Geula S et al. Stem cells. m6A mRNA methylation facilitates resolution of naive pluripotency toward differentiation. Science 347, 1002–1006 (2015). [PubMed: 25569111]
68. Rai K et al. Dnmt2 functions in the cytoplasm to promote liver, brain, and retina development in zebrafish. Genes Dev. 21, 261–266 (2007). [PubMed: 17289917]
69. Varier RA et al. N6-methyladenosine (m6A) reader Pho92 is recruited co-transcriptionally and couples translation to mRNA decay to promote meiotic fitness in yeast. Elife 11. 10.7554/eLife.84034 (2022).
70. Zaccara S & Jaffrey SR A Unified Model for the Function of YTHDF Proteins in Regulating m(6)A-Modified mRNA. Cell 181,1582–1595.e1518 (2020). [PubMed: 32492408]
71. Bushkin GG et al. m6A modification of a 3' UTR site reduces *RME1* mRNA levels to promote meiosis. Nat. Commun 10, 3414 (2019). [PubMed: 31363087]
72. Bodi Z, Bottley A, Archer N, May ST & Fray RG Yeast m6A Methylated mRNAs Are Enriched on Translating Ribosomes during Meiosis, and under Rapamycin Treatment. PLoS ONE 10, e0132090 (2015). [PubMed: 26186436]
73. Richard ML, Nobile CJ, Bruno VM & Mitchell AP *Candida albicans* biofilm-defective mutants. Eukaryot. Cell 4, 1493–1502 (2005). [PubMed: 16087754]
74. Jung JH & Kim J Roles of Edc3 in the oxidative stress response and CaMCA1-encoded metacaspase expression in *Candida albicans*. FEBS J. 281, 4841–4851 (2014). [PubMed: 25158786]
75. He PC & He C m6A RNA methylation: from mechanisms to therapeutic potential. EMBO J. 40, e105977, 10.15252/embj.2020105977 (2021). [PubMed: 33470439]
76. Yang C et al. The role of m6A modification in physiology and disease. Cell Death Dis. 11, 960 (2020). [PubMed: 33162550]
77. Yadav PK & Rajasekharan R The m6A methyltransferase Ime4 and mitochondrial functions in yeast. Curr. Genet 64, 353–357 (2018). [PubMed: 28975387]
78. Clancy MJ, Shambaugh ME, Timpte CS & Bokar JA Induction of sporulation in Saccharomyces cerevisiae leads to the formation of N6-methyladenosine in mRNA: a potential mechanism for the activity of the *IME4* gene. Nucleic Acids Res. 30, 4509–4518 (2002). [PubMed: 12384598]
79. Lee Y, Puumala E, Robbins N & Cowen LE Antifungal drug resistance: molecular mechanisms in *Candida albicans* and beyond. Chem. Rev 121, 3390–3411 (2021). [PubMed: 32441527]
80. Odds FC, Brown AJ & Gow NA Antifungal agents: mechanisms of action. Trends Microbiol. 11, 272–279 (2003). [PubMed: 12823944]
81. Xie JL, Polvi EJ, Shekhar-Guturja T & Cowen LE Elucidating drug resistance in human fungal pathogens. Future Microbiol. 9, 523–542 (2014). [PubMed: 24810351]
82. Mortazavi A et al. Mapping and quantifying mammalian transcriptomes by RNA-Seq. Nat. Methods 5, 621–628 (2008). [PubMed: 18516045]
83. Love MI, Huber W & Anders S Moderated estimation of fold change and dispersion for RNA-seq data with DESeq2. Genome Biol. 15, 550 (2014). [PubMed: 25516281]
84. Boyle EI et al. GO::TermFinder-open source software for accessing Gene Ontology information and finding significantly enriched Gene Ontology terms associated with a list of genes. Bioinformatics 20, 3710–3715 (2004). [PubMed: 15297299]
85. Skrzypek MS et al. The Candida Genome Database (CGD): incorporation of Assembly 22, systematic identifiers and visualization of high throughput sequencing data. Nucleic Acids Res. 45, D592–D596 (2017). [PubMed: 27738138]

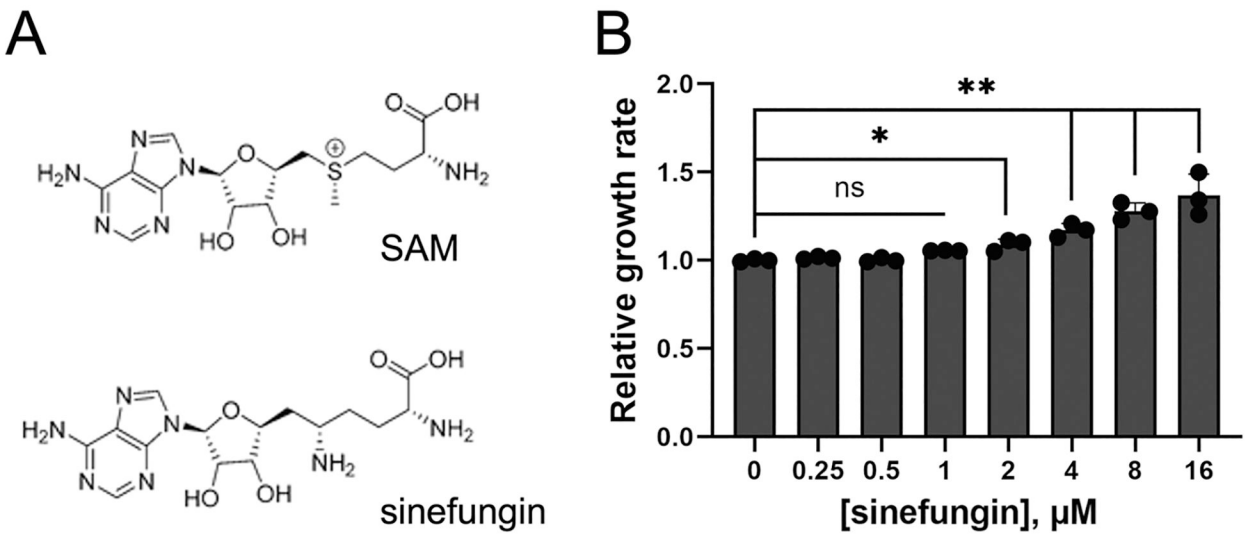

Fig. 1 |. Sinefungin does not inhibit 30 °C yeast growth at low concentrations.

A Structure of S-adenosylmethionine (SAM) alongside sinefungin, a SAM analog inhibitor of MTases. **B** Comparing the doubling time of SC5314 strain of *C. albicans* grown in YPD media with varying concentrations of sinefungin showed that sinefungin concentrations lower than 2 μM have no effect on the growth rate of *C. albicans*. Cells were incubated with the drug in a microplate reader at 30 °C for 24 h, with OD measured every 20 min. Doubling time was obtained from growth curve and normalized to no drug (0 μM) for relative growth rate. Error bars represent standard deviation (SD). ns: non-significant, $*P \leq 0.05$ and $**P \leq 0.01$.

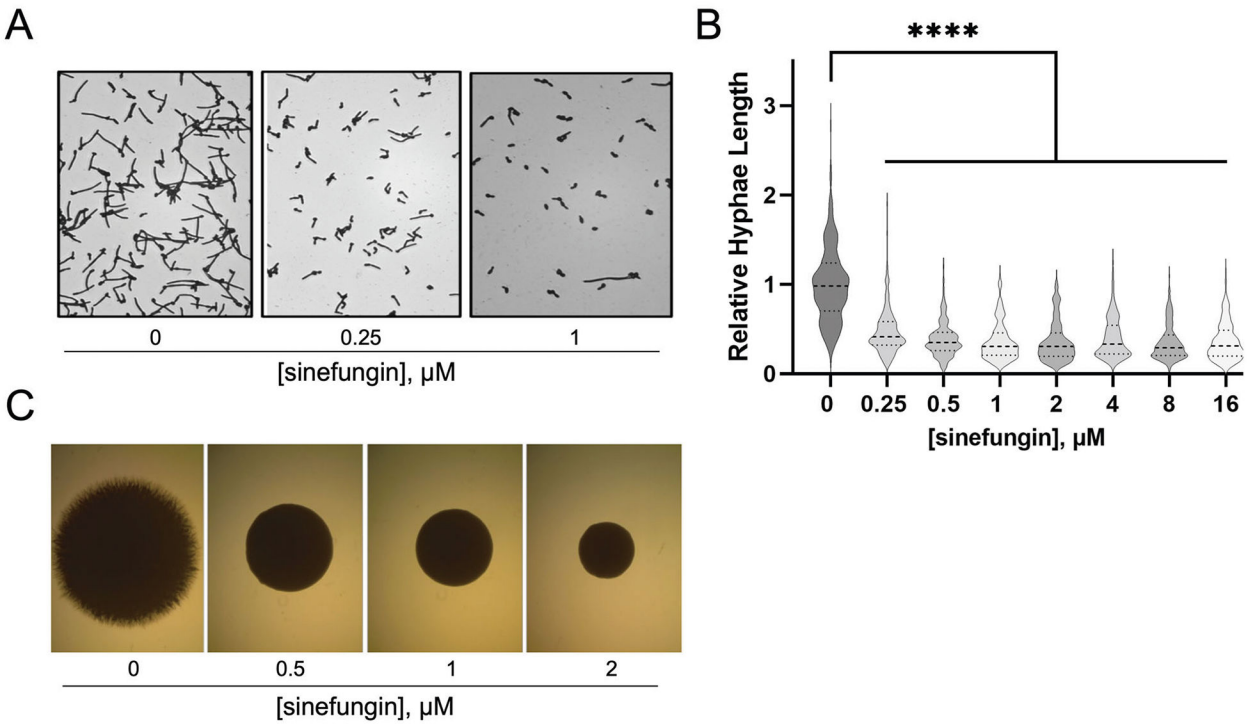

Fig. 2 |. Sinefungin inhibits morphological transition in *C. albicans* at concentrations that do not affect the growth of the yeast form.

A Representative images of data in 2B. **B** Hyphal morphogenesis. SC5314 was grown in RPMI-1640 at 37 °C + 10% FBS to induce hyphae formation with various sinefungin concentrations. After 2 h, cells were imaged on a plate reader and hyphae length was quantified using Image J software and normalized to no drug ($N = 250$). **C** Sinefungin inhibits long-term hyphae formation in *C. albicans*. SC5314 cells were plated onto solid Spider media agar plates containing various concentrations of sinefungin and incubated at 37 °C for 5 days before imaging. **** $P \leq 0.0001$.

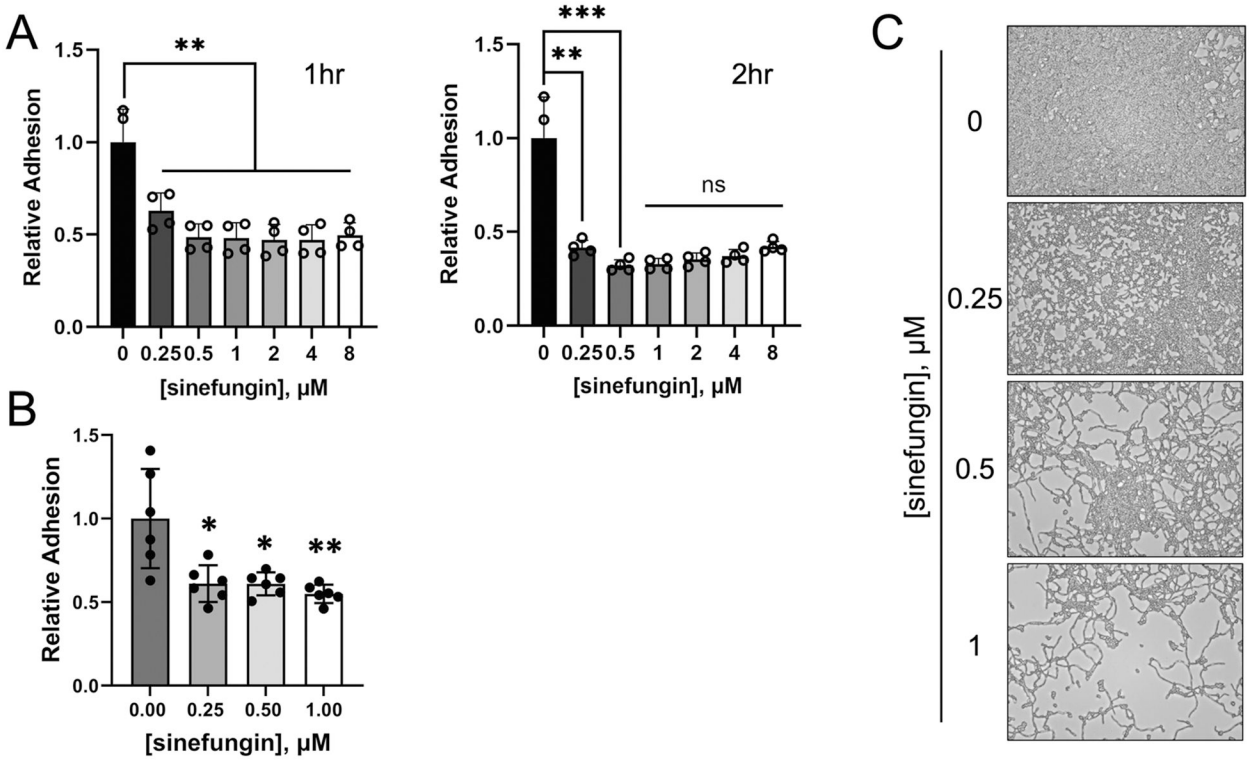

Fig. 3 |. Sinefungin impairs surface adhesion to polystyrene, hindering biofilm formation.
A Sinefungin impairs the short-term biofilm adhesion of *C. albicans*. SC5314 in RPMI-1640 was grown in a 96-well polystyrene plate with various concentrations of sinefungin. Plates were incubated at 37 °C with gentle shaking. At specific timepoints, plates were removed, and each well was washed with PBS to remove non-adherent cells. Adherent cells were immobilized with methanol and stained with crystal violet. Absorbance readings from a microplate reader were used to quantify early biofilm biomass, and biomass values were normalized to the no drug (0 μM) to determine relative adhesion of each treated group. Timepoints shown are 1 h and 2 h. **B** Sinefungin causes biofilm reversal and impaired surface adhesion after long-term biofilm formation by *C. albicans*. *C. albicans* biofilm was formed at 37 °C for 1.5 h in a 96-well polystyrene plate in Spider medium then treated with various concentrations of sinefungin for an 18-h incubation period at 37°C. Biofilm biomass was quantified using crystal violet and normalized to no drug for relative adhesion. **C** Representative images of data in 3B. Error bars represent SD. ns: non-significant, $*P \leq 0.05$, $**P \leq 0.01$, and $***P \leq 0.001$.

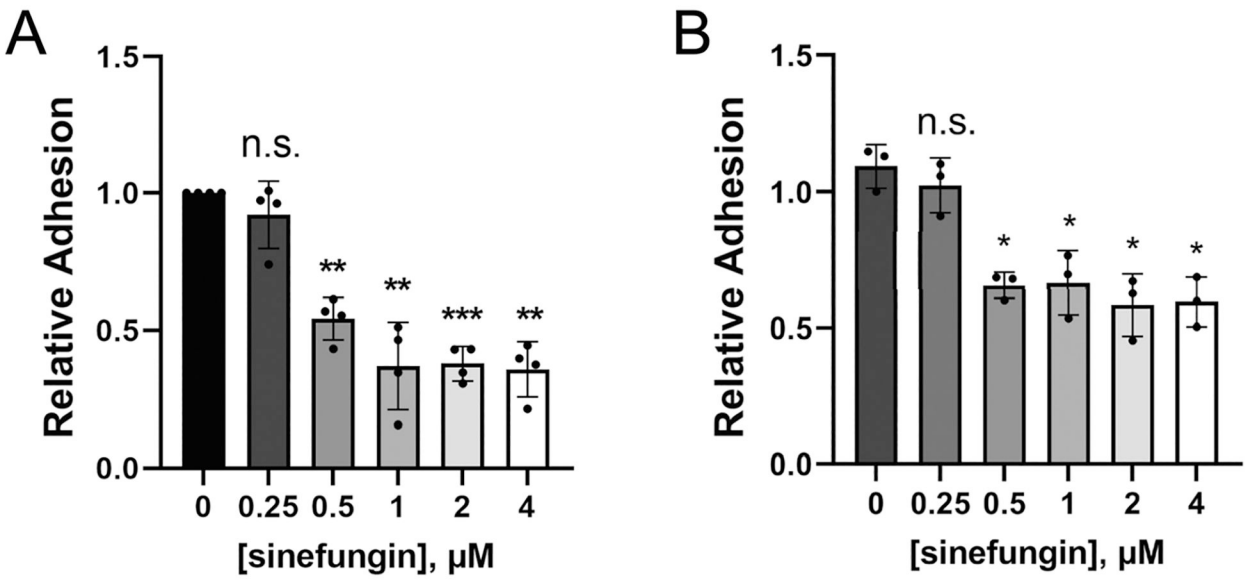

Fig. 4 |. *C. albicans* treated with low concentrations of sinefungin show reduced adhesion to human epithelial cell lines.

The adhesion of SC5314 strain of *C. albicans* to H1299 (**A**) and HEK293T (**B**) was measured in the presence of varying concentrations of sinefungin. Error bars represent SD. ns: non-significant, $*P \leq 0.05$, $**P \leq 0.01$, and $***P \leq 0.001$.

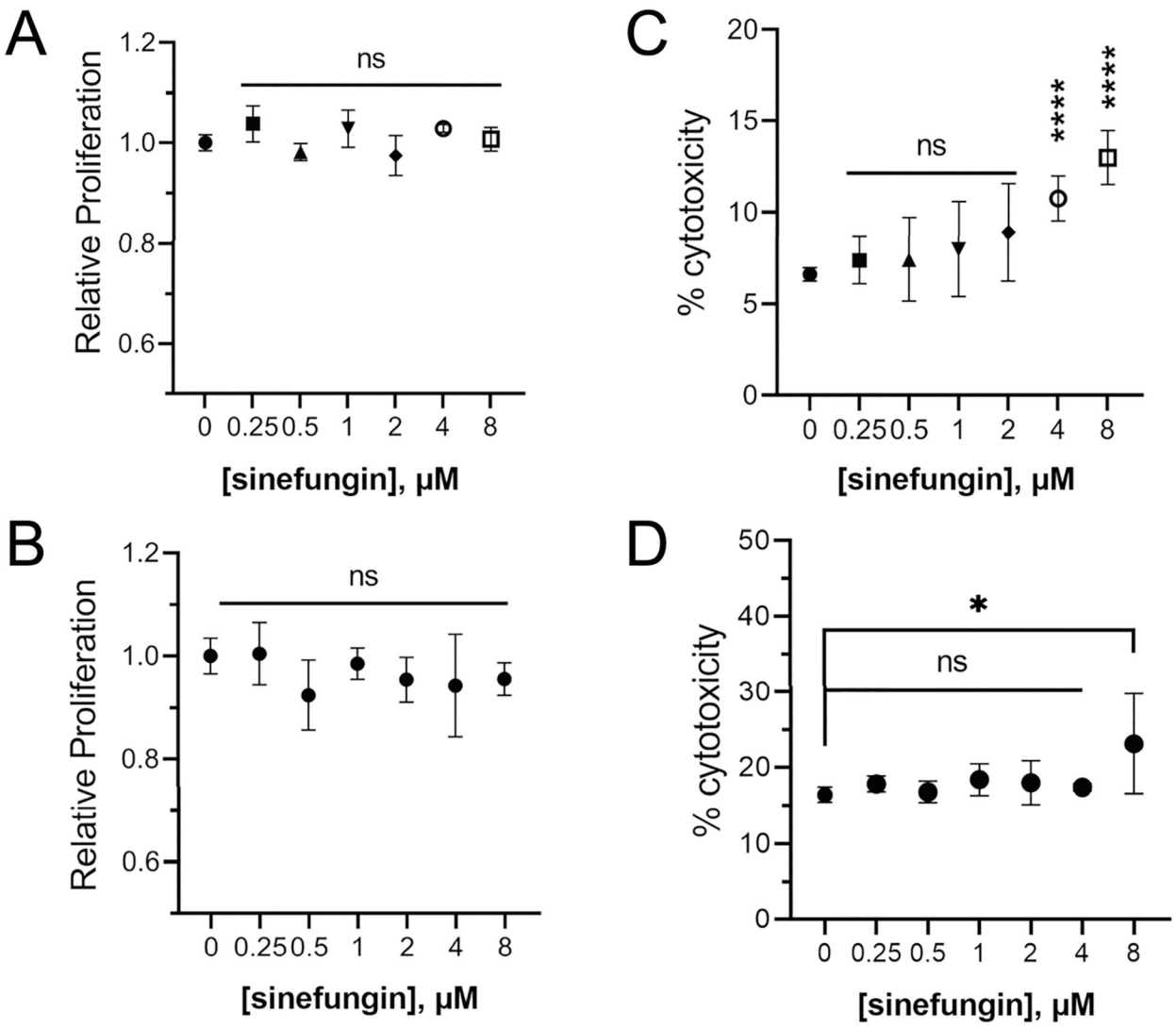

Fig. 5 |. Low concentrations of sinefungin have no effect on human epithelial cell viability.

A The metabolic activity of human epithelial cell lines H1299 (**A**) and HEK293T (**B**) was measured in presence of varying concentrations of sinefungin using a cell proliferation assay kit. Toxicity of different concentrations of sinefungin towards human cell lines H1299 (**C**) and HEK293T (**D**) was measured through an LDH assay. Lysed cells were used as a reference for 100% cytotoxicity, which all values were normalized to. Error bars represent SD. ns: non-significant, $*P \leq 0.05$ and $****P \leq 0.0001$.

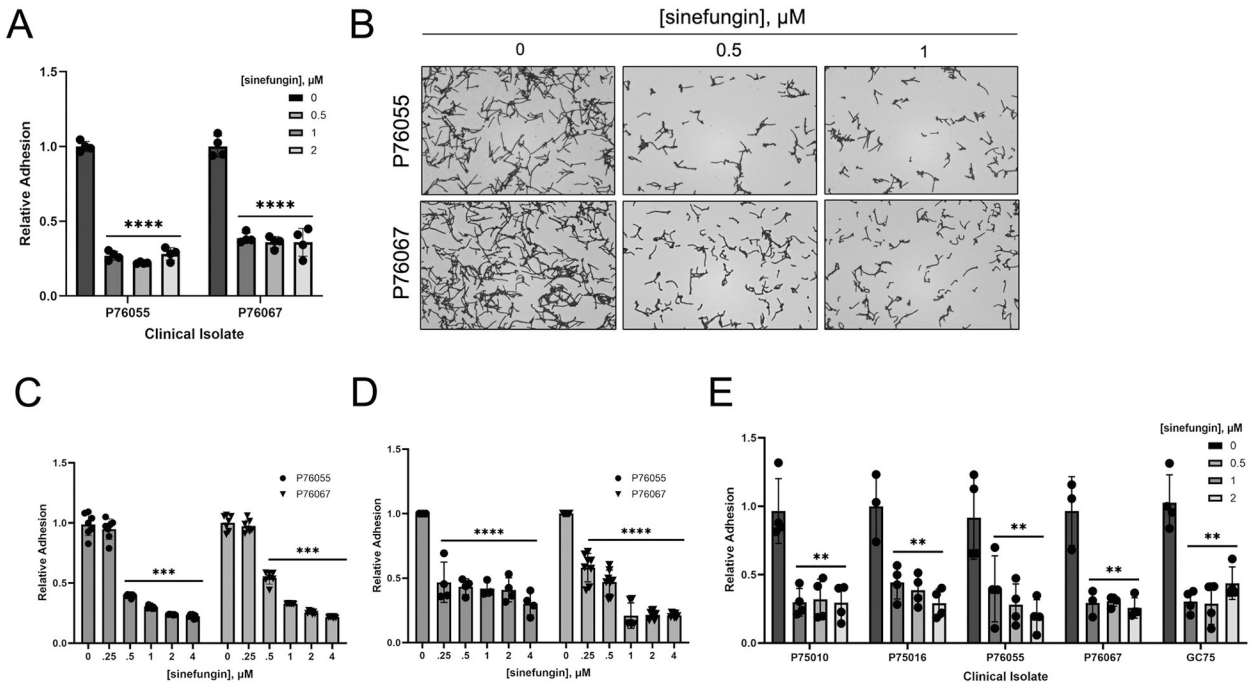

Fig. 6 |. Sinefungin impairs *C. albicans* clinical isolate hyphal growth, short-term and long-term surface adhesion, and adhesion to human epithelial cells.

A Sinefungin impairs the short-term biofilm adhesion of *C. albicans* clinical isolates. Two strains, P76055 and P76067, in RPMI-1640 were grown in 96-well polystyrene plates with various concentrations of sinefungin. Plates were incubated at 37 °C for 2 h with gentle shaking. At specific timepoints, plates were removed, and each well was washed with PBS to remove non-adherent cells. Adherent cells were immobilized with methanol and stained with crystal violet. Absorbance readings from a microplate reader were used to quantify early biofilm biomass, and biomass values were normalized to no drug (0 μM) to determine relative adhesion of each treated group. **B** Representative images of data in Fig. 6A. **C**, **D** Sinefungin inhibits adhesion of *C. albicans* clinical isolates to human epithelial cells. The adhesion of two *C. albicans* clinical isolates, P76055 and P76067, to H1299 (**C**) and HEK293 (**D**) was measured in the presence of varying concentrations of sinefungin. **E** Sinefungin causes biofilm reversal and impaired surface adhesion after long-term biofilm formation by *C. albicans* clinical isolates. Biofilms of five strains, P75010, P75016, P76055, P76067, and GC75, were formed at 37 °C for 1.5 h in 96-well polystyrene plates in Spider medium then treated with various concentrations of sinefungin for an 18-h incubation period at 37 °C. Biofilm biomass was quantified using crystal violet and normalized to no drug for relative adhesion. Error bars represent SD. $^{**}P \leq 0.01$, $^{***}P \leq 0.001$ and $^{****}P \leq 0.0001$.

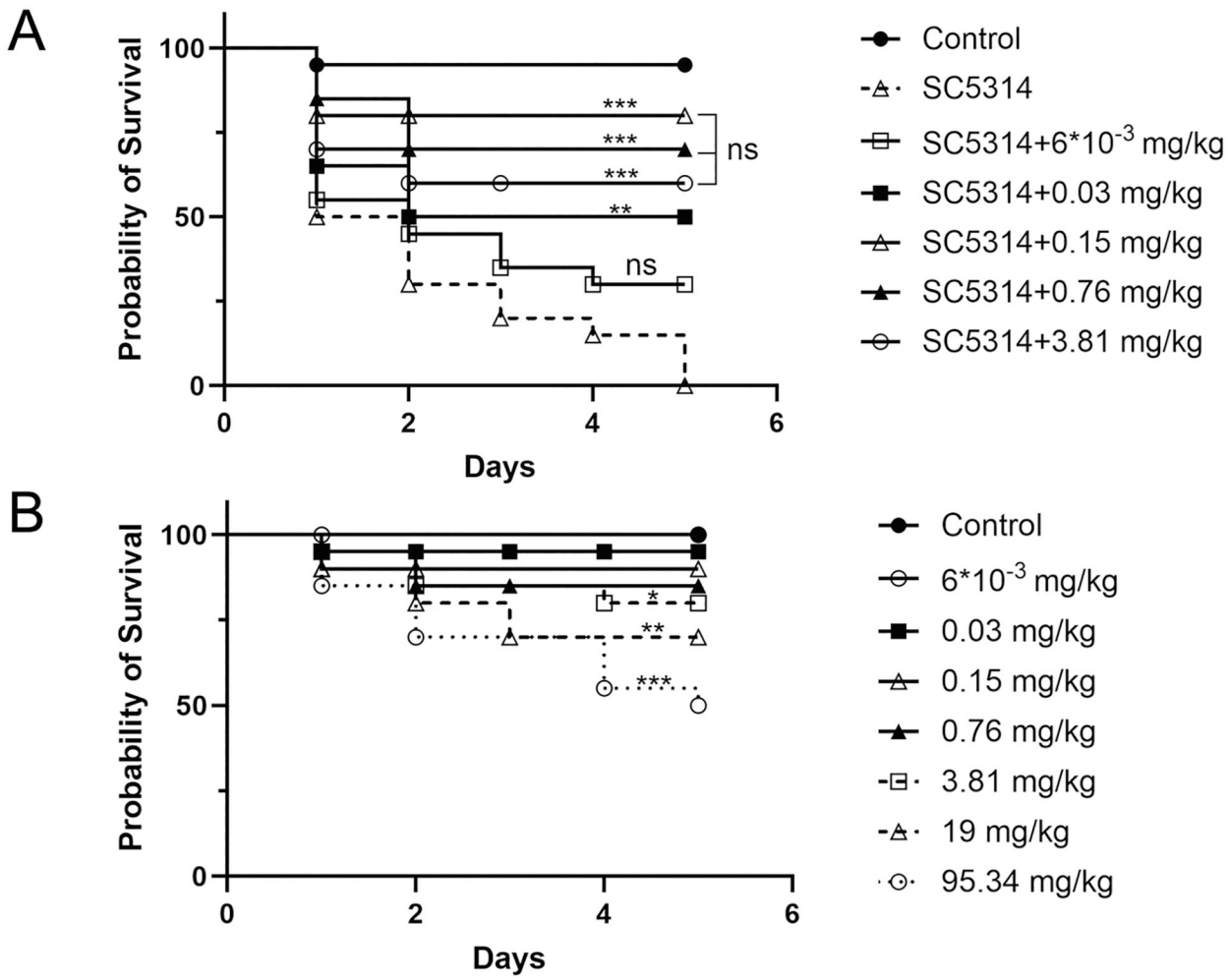

Fig. 7 |. Sinefungin inhibits virulence of *C. albicans* in *G. mellonella* infection model at biologically non-toxic concentrations.

A Sinefungin suppresses *C. albicans* infection in *G. mellonella* at concentrations between 0.15 and 3.81 mg/kg. Healthy *G. mellonella* larvae were inoculated with 1×10^5 CFU/larva of SC5314 cells, with a control group receiving 10 μL of PBS, and 1 h after inoculation, various concentrations of sinefungin were administered via injection. Daily mortality rates were recorded over a 5-day observation period. **B** Sinefungin has no toxic effects against *G. mellonella* at concentrations of 0.76 mg/kg or lower. *G. mellonella* larvae were administered various concentrations of sinefungin, with a control group receiving 10 μL of PBS. Daily mortality rates were recorded over a 5-day observation period. Survival curves were compared with the Log-rank (Mantel-Cox) test. ns: non-significant, $*P \leq 0.05$, $**P \leq 0.01$, and $***P \leq 0.001$.

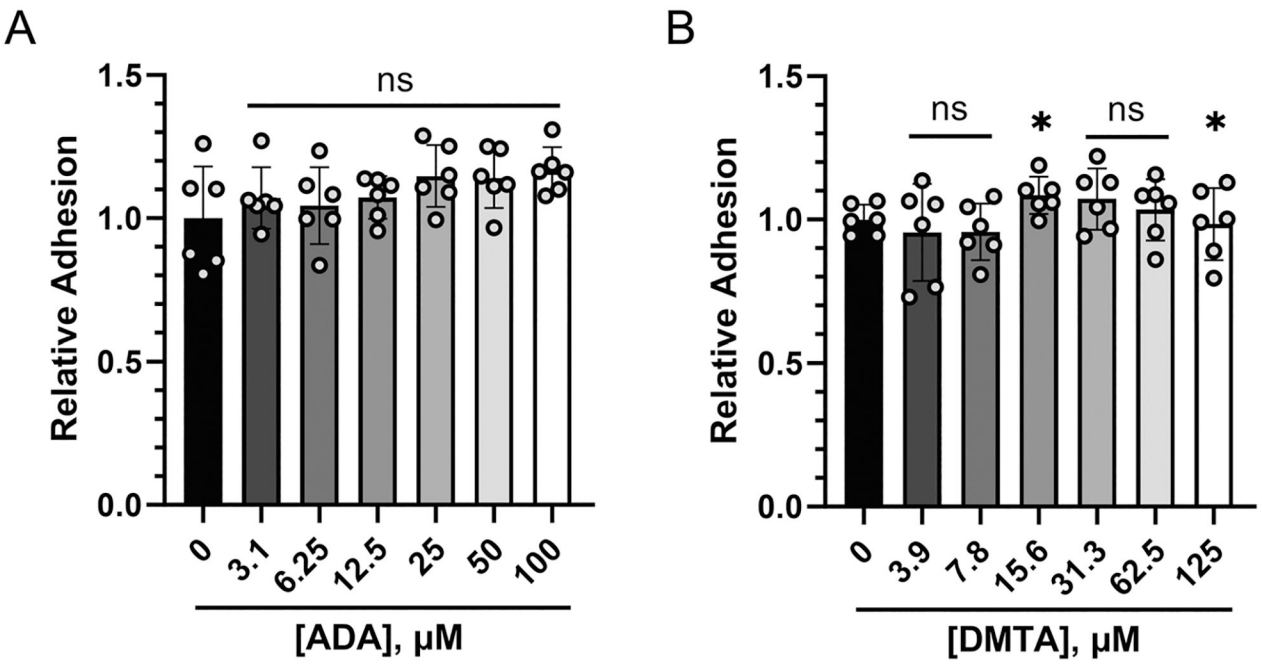

Fig. 8 |. Alternative SAM-analog MTase inhibitors have no consistent effect on surface adhesion and early biofilm formation on polystyrene.

SC5314 strain *C. albicans* cells were incubated for 3 h at 37 °C in RPMI-1640 with (**A**) adenosine dialdehyde (ADA) and (**B**) 5'-deoxy-5'-methylthioadenosine (DMTA) concentrations diluted in 1% DMSO before measuring the biofilm mass using crystal violet. Error bars represent SD. ns: non-significant, $*P \leq 0.05$.

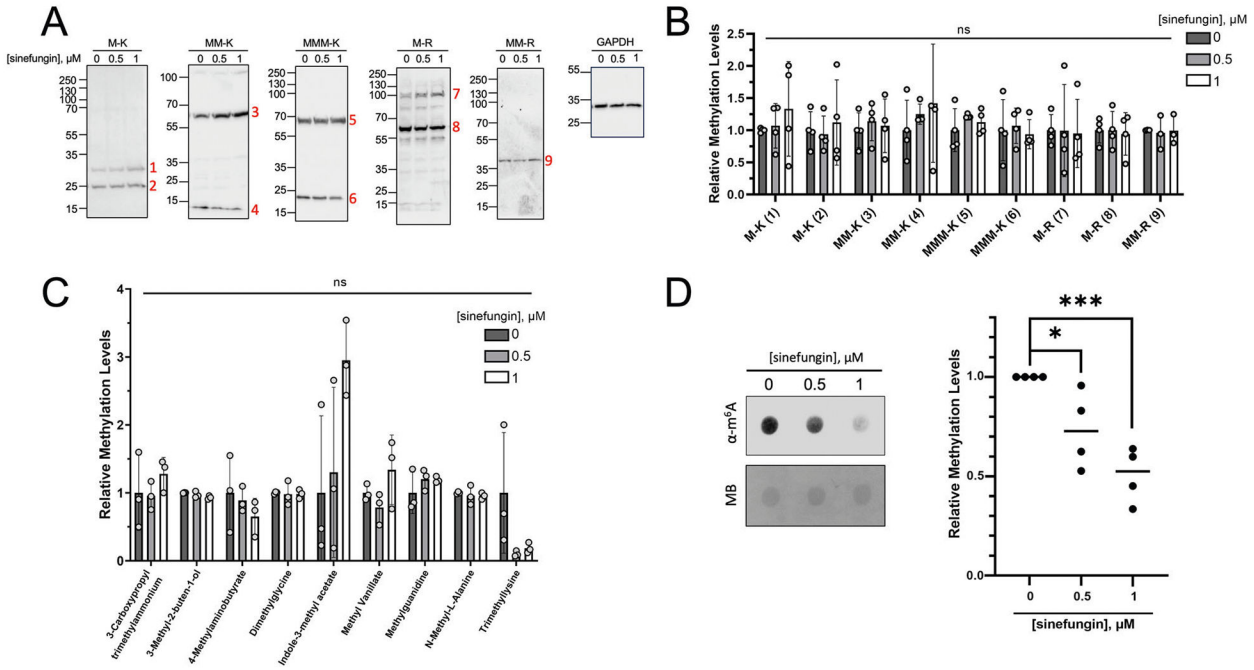

Fig. 9 |. m^{6}A modifications in RNA are significantly reduced in *C. albicans* exposed to 1 μM or less of sinefungin.

A Representative images of data in Fig. 9B. Bands are numbered according to corresponding quantification data in Fig. 9B (i.e., Band 1 corresponds to M-K (1) on graph). **B** The major methylated proteins in the hyphae form of *C. albicans* are unaffected by sinefungin. SC5314 cells were grown in hyphae form in the presence of varying concentrations of sinefungin. Cells were lysed, and total protein was extracted for western blot. Lysine and arginine methylation levels were probed with respective pan-methyl antibodies and quantified in ImageLab. Quantification data was normalized to both loading control and zero drug. **C** Hyphal metabolite methylation levels are unaffected by sinefungin. SC5314 cells were grown in hyphae form in the presence of no drug, 0.5 μM and 1 μM of sinefungin. Metabolite methylation levels were analyzed using LC-MS/MS. **D** RNA m^{6}A levels are reduced in the presence of sinefungin. SC5314 cells were grown in hyphae form with varying concentrations of sinefungin. The m^{6}A levels were measured using dot blot using an anti-m^{6}A antibody. The equal loading of the RNA was assessed using methylene blue (MB). Error bars represent SD. ns: nonsignificant, *$P \leq 0.05$ and ***$P \leq 0.001$.

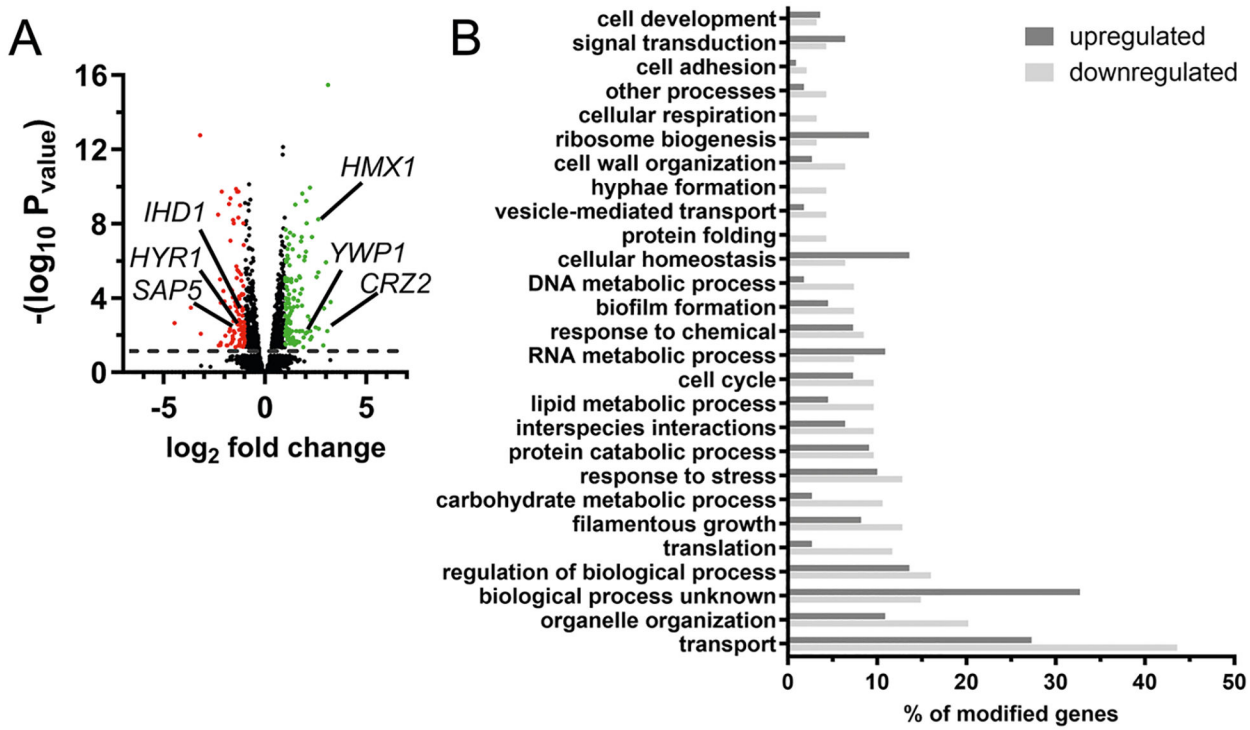

Fig. 10 |. Overall transcriptomic changes of *C. albicans* grown under hyphae-inducing conditions in response to sinefungin treatment.

A SC5314 cells were grown in hyphae form in the presence or absence of 1 μM sinefungin and total RNA was extracted and sequenced. Significantly downregulated (red) and upregulated (green) genes in samples treated with sinefungin are shown on a volcano plot. A cutoff absolute value of $\log_2$ fold change >1 (2-fold change) was used. Adjusted $P < 0.05$. Several examples of genes associated with pathogenicity of *C. albicans* are marked on the plot. **B** Bar graph representation of significantly overrepresented Gene Ontology terms for biological processes with up- or down-regulated genes in response to treatment with 1 μM sinefungin.